Journal of Orthopaedic Translation 49 (2024) 308–324

Contents lists available at ScienceDirect

Journal of Orthopaedic Translation

journal homepage: www.journals.elsevier.com/journal-of-orthopaedic-translation

Original Article

Zhuangyao Jianshen Wan ameliorates senile osteoporosis in SAMP6 mice through Modulation of the GCN5L1-mediated PI3K/Akt/wnt signaling pathway

Shaoyong Ma [a,b,1], Jian Lin [a,1], Meng Yang [a,1], JiaJia Wang [c,1], Lujiao Lu [d], Ying Liang [e], Yan Yang [a], Yanzhi Liu [f,**], Dongtao Wang [g,h,***], Yajun Yang [a,*]

[a] Department of Pharmacology, School of Ocean and Tropical Medicine, Guangdong Medical University, Zhanjiang 524023, Guangdong, China
[b] The Second Affiliated Hospital, Guangdong Medical University, Zhanjiang 524023, Guangdong, China
[c] School of Traditional Chinese Medicine, Zhanjiang University of Science and Technology, Zhanjiang 524094, Guangdong, China
[d] Affiliated Hospital, Guangdong Medical University, Zhanjiang 524023, Guangdong, China
[e] School of Women and Children's Medicine, Guangdong Medical University, Zhanjiang 524023, Guangdong, China
[f] Zhanjiang Key Laboratory of Orthopaedic Technology and Trauma Treatment, Key Laboratory of Traditional Chinese Medicine for the Prevention and Treatment of Infectious Diseases, Zhanjiang Central Hospital, Guangdong Medical University, Zhanjiang 524037, China
[g] Department of Traditional Chinese Medicine, Shenzhen Hospital, Southern Medical University, Shenzhen 518000, Guangdong, China
[h] School of Traditional Chinese Medicine, Southern Medical University, Guangzhou 510000, Guangdong, China

ARTICLE INFO

Keywords:
GCN5L1
PI3K/Akt
Senile osteoporosis
Wnt/β-catenin
Zhuangyao jianshen wan

ABSTRACT

Background: Senile osteoporosis (SOP) is a systemic bone disease characterized by increased susceptibility to fractures. However, there is currently no effective treatment for SOP. The Zhuangyao Jianshen Wan (ZYJSW) pill is traditionally believed to possess kidney-nourishing and bone-strengthening effects, demonstrating efficacy in treating fractures. Despite this, its effectiveness and mechanism in SOP remain unclear. This study aims to investigate the therapeutic potential of ZYJSW in treating SOP in senescence accelerated mouse prone 6 (SAMP6, P6) mice, and elucidate the underlying mechanisms.

Methods: Four-month-old SAMP6 mice were categorized into six groups: the model group (SAMP6), low, medium, and high-dose ZYJSW treatment groups, calcitriol treatment (positive control 1) group, and metformin treatment (positive control 2) group. Gastric administration was carried out for 15 weeks, and a normal control group comprising four-month-old Senescence-Accelerated Mouse Resistant 1 (SAMR1) mice. Changes in body weight, liver and kidney function, bone protective effects, and muscle quality were evaluated using various assays, including H&E staining, Goldner staining, bone tissue morphology analysis, Micro-CT imaging, and biomechanical testing. Qualitative analysis and quality control of ZYJSW were performed via LC-MS/MS analysis. To explore mechanisms, network pharmacology and proteomics were employed, and the identified proteins were validated by Western blotting.

Results: Oral administration of ZYJSW to P6 mice exerted preventive efficacy against osteopenia, impaired bone microstructure, and poor bone and muscle quality. ZYJSW attenuated the imbalance in bone metabolism by promoting bone formation, as evidenced by the upregulation of key factors such as Runt-related transcription factor 2 (RUNX2), Bone Morphogenetic Protein (BMP2), Osteoprotegerin (OPG) and Osteocalcin (OCN), while simultaneously inhibiting bone resorption through the downregulation of TNF receptor associated factor 6 (TRAF6), Tartrate resistant acid phosphatase (TRAP), Receptor activator for nuclear factor-κB ligand (RANKL) and Cathepsin K (CTSK). Additionally, ZYJSW enhanced muscle structure and function by counteracting the elevation of Ubiquitin (Ub), Muscle RING-finger protein-1 (Murf-1), F-Box Protein 32 (FBOX32), and Myogenin (Myog). Network pharmacology predictions, proteomics analysis corroborated by published literature demonstrated the role of ZYJSW involving in safeguarding mitochondrial biogenesis. This was achieved by suppressing

* Corresponding author.
** Corresponding author.
*** Corresponding author. Department of Traditional Chinese Medicine, Shenzhen Hospital, Southern Medical University, Shenzhen 518000, Guangdong, China
E-mail addresses: liuyanzhi02@163.com (Y. Liu), 95401864@qq.com (D. Wang), yangyajun1@163.com (Y. Yang).
[1] Shaoyong Ma, Jian Lin, Meng Yang and JiaJia Wang contributed equally to this work.

https://doi.org/10.1016/j.jot.2024.08.009
Received 6 March 2024; Received in revised form 12 June 2024; Accepted 8 August 2024

GCN5L1 expression, contributing to the heightened expression of TFAM, PGC-1α, and nuclear respiratory factor-1 (NRF-1) proteins. ZYJSW also positively modulated Wnt signaling pathways responsible for bone formation, due to regulating expressions of key components like β-catenin, GSK-3β, and LRP5. In addition, ZYJSW causes the downregulation of the PI3K/Akt pathway by inhibiting the phosphorylation of both PI3K and Akt.
Conclusions: The study highlights the significance of ZYJSW in preserving the health of both bone and muscle in P6 mice, potentially through the regulation of the GCN5L1-mediated PI3K/Akt/Wnt signaling pathway.
The translational potential of this article: Our research provides evidence and a mechanistic rationale for ZYJSW as a candidate for SOP treatment, offering insights for further exploration and strategy development.

1. Introduction

SOP is a systemic bone disease characterized by an increased susceptibility to fractures, diminished bone mass, compromised bone microstructure, heightened bone fragility, and an elevated risk of fractures [1]. Over the past 40 years, with the rising life expectancy and an aging population, SOP patients have reached 110 million [2]. Given its subtle symptoms, severe consequences, and the challenges associated with delayed diagnosis and treatment, the early prevention, diagnosis, and treatment of SOP are critical in an aging society. Currently, pharmacological treatments for SOP mainly include expensive and inconvenient parathyroid hormone, along with calcium supplements and vitamin D, which exhibit modest efficacy [3]. These limitations reinforce the urgent need to develop new, safe drugs for SOP, with the goal of reducing the loss of bone and muscle and enhancing the quality of life for the elderly.

The accelerated functional decline in bone metabolism with aging involves a decrease in mitochondrial biogenesis, a process crucial for osteoblast differentiation [4,5]. Inreasing documents highlight the association of mitochondrial biogenesis with GCN5L1, a significant protein with a sequence homologous to the nuclear acetyltransferase GCN5 [6]. GCN5L1 regulates various mitochondrial functions, such as fatty acid oxidation and gluconeogenesis [7,8]. The loss of GCN5L1 induces the expression of PGC-1α and initiates mitochondrial biogenesis [9,10]. In osteoblast differentiation, mitochondrial biogenesis is promoted by upregulating PGC-1α, NRF-1, and TFAM, facilitating ATP production [9,11]. Moreover, mitochondrial function, promoting β-catenin acetylation, is involved in the Wnt pathway responsible for osteogenic differentiation [12]. Recently, GCN5L1 is implicated in the PI3K/Akt pathway and participates in the Wnt signaling by regulating mitochondrial biogenesis [13]. The PI3K/Akt pathway is crucial for maintaining bone metabolism. In the skeletal system, phosphorylated AKT inhibits GSK-3β-induce degradation of β-catenin, leading to the upregulation of the Wnt pathway and fostering bone formation. These pieces of evidence suggest a signaling crosstalk between the PI3K/Akt and Wnt pathways [14]. Overall, the regulation of mitochondrial biogenesis by GCN5L1 may represent a novel mechanism for treating SOP.

In Traditional Chinese Medicine (TCM), SOP is classified under terms like “bone atrophy”. Throughout life, skeletal tissues undergo a transition from strength to weakness with aging, reflecting patterns observed in SOP. The Huangdi Neijing emphasizes the crucial role of the Kidneys in nourishing bones, stating that Kidney “govern bones” and “nourishes bone marrow." If Kidney Qi, as an essential life substance, is deficient, bones become susceptible to weakness and fractures, in accordance with the theory that “Kidney deficiency leads to bone weakness." Kidney deficiency, therefore, emerges as a pivotal factor in the development of SOP. Addressing Kidney deficiency is foundational in SOP treatment, with formulations like the Zhuangyao Jianshen Wan (ZYJSW) pill, a Tang Dynasty formula known for nourishing Kidneys [15]. The formula comprises nine herbs, including *Cibotium barometz* (Gou Ji), *Kadsura coccinea* (Hei Lao Hu), *Taxillus Herba* (Sang Ji Sheng), *Millettia speciosa champ* (Niu Da Li), *Ligustrum lucidum* (Nv Zhen Zi), *Cuscuta chinensis* (Tu Si Zi), *Rosa laevigata Michx* (Jing Ying Zi), *Flemingia Roxb* (Qian Jin Ba), and *Spatholobi Caulis* (Ji Xue Ten) (Table 1). These herbs work together to invigorate the kidney function, activate blood circulation, and resolve stasis. *C. barometz* and *C. chinensis* seed nourish the liver and kidneys, strengthen tendons and bones, and are considered the Sovereign herbs. *Taxillus Herba* and *L. lucidum* nourish the kidneys and strengthen bones, while *M. speciosa champ* dispels wind and activates collaterals, serving as ministerial herbs. *Spatholobi Caulis* and *K. coccinea* supplement blood and invigorate blood circulation, while *Flemingia Roxb R. laevigata Michx* essence and controls urination, acting as assistant herbs [16]. Among these herbs, *C. barometz*, *L. lucidum*, *Spatholobi Caulis, C. chinensis*, *Taxillus Herba*, *Flemingia Roxb* and *M. speciosa champ* have been found to regulate bone metabolism and treat osteoporosis [17]. *C. barometz*, *L. lucidum* and *Spatholobi Caulis* inhibit the activity of osteoclasts and promote the differentiation of osteoblasts. *C. chinensis*, *Taxillus Herba* and *Flemingia Roxb* promote the proliferation and differentiation of osteoblasts [18–20]. *M. speciosa champ* also inhibits the activity of osteoclasts [21]. ZYJSW is celebrated for the remarkable capacity to nourish kidney yang, enhance kidney essence, and strengthen bones. It has been reported that ZYJSW has antioxidant and anti-aging effects, and it has the ability to promote the healing of compressive vertebral fractures in SOP [17]. Muscles and bones are intricately linked, and the onset of osteopenia during aging coincides with the simultaneous loss of muscle mass, aligning with TCM’s “Weizheng” [22]. Further research is crucial to investigate the efficacy of ZYJSW in improving both bone and muscle quality through kidney nourishment in SOP (Table 2).

This study aimed to explore the efficacy of ZYJSW in treating SOP using the rapid aging model of SAMP6 mice, recognized as nevol SOP animal model. This model exhibits characteristics such as increased bone fragility, degraded bone microstructure, loss of bone matrix, and abnormal metabolism and dysfunction of bone cell [23]. In addition, this study sought to elucidate the underlying mechanism of action through network pharmacology and proteomics, and to validate by Western blotting in P6 mice. The results of this study provide an experimental foundation for a better understanding of SOP’s pathogenesis and the development of novel therapeutic strategies.

2. Materials and methods

2.1. Administration sample preparation

ZYJSW was purchased from Guangzhou Baiyunshan Chenliji Co., Ltd. (NO: A08169). The preparation extraction involved soaking in warm water for 20 min followed by 10 min of ultrasound treatment. For administration, the clinical recommended dosage of ZYJSW is three times a day, with 3.5 g each time. The ratio of clinical dosage between

Table 1
ZYJSW ingredients.

Chinese Names	Herb Names in Latin	Abbreviations	Prescription Analysis
Gou Ji	*Cibotium barometz*	GJ	Sovereign herbs
Hei Lao Hu	*Kadsura coccinea*	HLH	Adjuvant herbs
Nv Zhen Zi	*Ligustrum lucidum*	NZZ	Minister herbs
Qian Jin Ba	*Flemingia Roxb*	QJB	Adjuvant herbs
Ji Xue Teng	*Spatholobi Caulis*	JXT	Adjuvant herbs
Jin Ying Zi	*Rosa laevigata Michx*	JYZ	Adjuvant herbs
Tu Si Zi	*Cuscuta chinensis*	TSZ	Sovereign herbs
Niu Da Li	*Millettia speciosa champ*	NDL	Minister herbs
Sang Ji Sheng	*Taxillus Herba*	SJS	Minister herbs

Table 2
LC-MS/MS data.

Serial number	Retention time (min)	Chinese name	English name	Structural formula
1	1.1	原儿茶酸	Protocatechuic acid	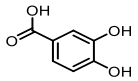
2	2.2	原儿茶醛	3,4-Dihydroxybenzaldehyde	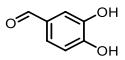
3	3.3	绿原酸	Chlorogenic acid	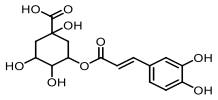
4	4.3	咖啡酸	Caffeic acid	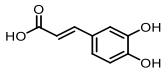
5	8.04	长寿花糖苷	Corchoionoside C	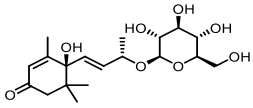
6	10.5	金丝桃苷	Hyperoside	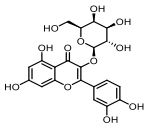
7	10.6	异槲皮苷	Isoquercitrin	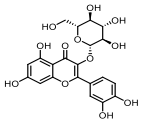
8	11.0	特女贞苷	Protocatechuic acid	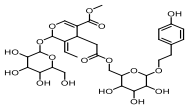
9	11.4	紫云英苷	Astragalin	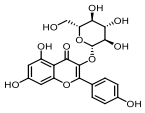
10	12.5	槲皮素	Quercetin	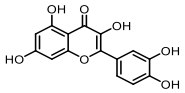
11	13.7	山奈酚	Kaempferol	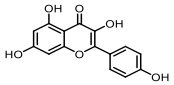

mice and humans is 8.75 mg/kg. Converted to mouse dosages, the medium dose is set at 1.53 g/kg, with the high and low doses being double and half of the medium dose, respectively, at 3.06 g/kg and 0.765 g/kg [24]. Metformin (dimethylbiguanide) was purchased from Sino-American Shanghai Sino-American Pharmaceutical Co., Ltd. (NO: H20023370), was prepared at a concentration of 20 mg/ml by dissolving it in 25 ml of distilled water using ultrasound. Rosiglitazone capsules were obtained from Shanghai Roche Pharmaceuticals (NO: B4140), each containing 0.25 μg. A suspension of 0.5 % CMC-Na (50 ml) was prepared for administration by dissolving the capsule. The administration involved gastric gavage with 0.1 ml of a 0.005 μg/ml rosiglitazone solution per 10g body weight.

2.2. Experimental animals

The experimental protocol was approved by the Ethics Committee of Guangdong Medical University on Laboratory Animal Care. Male SAMR1 mice and SAMP6 mice (Certificate: SCXK (jing) 2016-0010) were purchased from the Experimental Animal Science Department of Peking University. Four-month-old SAMP6 mice were categorized into six groups: the model group (P6), low (P6+L), medium (P6+M), and high-dose ZYJSW treatment groups (P6+H), calcitriol treatment group (positive control 1, P6+Cal), and metformin treatment group (positive control 2, P6+Met). Gastric administration was carried out for 15 weeks, with a normal control group comprising four-month-old SAMR1 mice

(R1). The mice were maintained at 25 ± 1 °C with a 12-h light–dark cycle, and provided with standard laboratory food and water ad libitum.

2.3. Collection of different Specimens

Calcein (24 mg/kg, Sigma, St. Louis, MO, USA) and calcein (7 mg/kg) was subcutaneously injected into all rats on d 13, 14, and d 3, 4 before sacrifice at the end point of experimental. The right femur was collected to assess bone biomechanical properties and microstructure. Proximal non-decalcified sections of the right tibia were used for bone histomorphometry analysis. Morphological analysis was performed on the liver, kidneys, right gastrocnemius muscle, and left femur using light microscopy.

2.4. Renal index, hepatic index, spleen index

Weights of the kidneys, spleen, and liver were measured, and organ indices were computed. The renal index, spleen index, and hepatic index were determined as the ratios of kidney weight, spleen weight, and liver weight to mouse body weight, respectively.

2.5. H&E staining, Masson-Goldner staining, toluidine blue staining

H&E staining was performed according to the instructions of the H&E staining reagent kit. Sections were deparaffinized, hydrated, stained with hematoxylin for 5 min, differentiated for 1 s, rinsed in running water for 1 min, stained with eosin for 30 s, and dehydrated and cleared before mounting with neutral gum. Masson-Goldner staining involved deparaffinization, hydration, iron hematoxylin and ponceau staining, differentiation in weak acid solution, green staining, dehydration, and mounting with neutral gum. Toluidine blue staining included toluidine blue staining for 1 min, rinsing in running water for 1 min, gradient ethanol dehydration, xylene transparency, and sealing with neutral gum. Microscopic observations and photography were performed.

2.6. BMD, Micro-CT, bone Biomechanics, and Morphometry

Using a Bruker X-ray scanner, mice underwent whole-body scanning at 40 kV, 3.40 s, and 0.20 mA. Measurements of bone mineral content (BMC) and calculation of bone density (BMD) were performed. Long bone mechanical strength was evaluated via three-point bending tests using an MTS testing machine. Micro-CT scanning determined the microstructure of trabecular bone at the proximal end of the right femur. 3D reconstructions of trabeculae provided parameters such as trabecular number (Tb.N), trabecular thickness (Tb.Th), bone volume fraction (BV/TV), and trabecular separation (Tb.Sp). Histomorphological analysis of the tibia, stained with toluidine blue, observed trabecular structure. Bone formation indicators, including double-fluorescent labeling parameters (%L.pm) and bone surface-based new bone formation rate (BFR/BS), were assessed using fluorescence labeling.

2.7. Serum Biomarker measurement

Following euthanasia, blood was collected and allowed to stand at 4 °C for 4 h before serum separation. Serum levels of PINP (bone formation markers), CTX-I (bone resorption markers), β-galactosidase (aging marker), and liver and kidney toxicity markers alanine transaminase (ALT), aspartate transaminase (AST), and serum creatinine (Scr).

2.8. Muscle enzyme activity measurement

About 0.1g of gastrocnemius muscle tissue was homogenized in 1 ml of ice-cold extraction buffer. Following centrifugation, the supernatant was collected for measuring Na^{+}-K^{+}-ATPase and Ca^{2+}-Mg^{2+}-ATPase activity. The enzyme activity was assessed using a spectrophotometer.

2.9. LC-MS/MS analysis

Chromatographic separation utilized an Agilent 1290 UPLC system with a Waters BEH C18 column (2.1 × 100 mm, 1.7 μm) and a mobile phase of 0.1 % formic acid in water and methanol. Detection was performed using ESI-MS/MS in positive and negative ion modes. Compounds such as protocatechuic acid, 3, 4-Dihydroxybenzaldehyde, chlorogenic acid, caffeic acid, roseoside, hyperoside, isoquercitrin, spcnuezhenide astragalin, quercetin and kaempferol were identified by matching with natural product reference standards. Compound data, including molecular weight, mass spectrometry fragmentation pattern, and relative retention time, were obtained.

2.10. Network pharmacology

Genecards and drug online databases were used with "senile osteoporosis" as the keyword to screen for disease targets. The TCMSP and SwissTargetPrediction databases were employed to predict the targets of active compounds in Zhuangyao Jianshen Wan. The Venn diagram was used to analyze the overlap between active compound targets and targets related to SOP. The protein–protein interaction (PPI) network was constructed using the String database, and core targets were obtained using the CytoHub plugin in Cytoscape 3.9.1. Gene Ontology (GO) and Kyoto Encyclopedia of Genes and Genomes (KEGG) enrichment analyses were performed using the Metascape database.

2.11. Proteomics

Left tibia samples were collected, and unlabeled quantitative proteomics technology was used, developed by Shanghai Baishu Biomedical Technology Co., Ltd. Bioinformatics analysis methods such as volcano analysis, subcellular localization prediction, GO annotation enrichment analysis, and KEGG annotation enrichment analysis were used to explore the pathogenesis of SOP in SAMP6 mice.

2.12. Western Blot

Protein was extracted with lysis buffer. Sodium dodecyl sulfate-polyacrylamide gel electrophoresis (SDS-PAGE) was performed, and proteins were transferred to polyvinylidene fluoride (PVDF) membranes. Membranes were blocked, incubated with primary antibodies GSK-3β (SAB#48798), β-catenin (ab32572), RUNX2 (ab236639), OCN (ab133612), BMP2 (ab214821), TFAM (SAB#29688), OPG (SAB#48798), PGC-1α (SAB#29688), TRAP (NBP2-01026), p-GSK-3β (SAB#11002), GCN5L1 (SAB#30754), LRP5 (AF4645#), RANKL (AF0313), IL-11 (AF5211), NRF-1 (SAB#27194), p-β-catenin (SAB#14002), TRAF6 (ab40675), CTSK (ab19027), GSK-3β (SAB#48798), washed, and then incubated with secondary antibodies. Protein expression was detected using the FlourChem Q imaging system, and quantitative analysis was performed using Image-Pro Plus software.

2.13. Statistical analysis

Analysis of variance (ANOVA) was performed using SPSS 24.0 for assessing the effects of various treatments, assuming normal distribution and equal variance. When $p > 0.05$, the data were considered normally distributed. When $p > 0.05$ for heterogeneity of variance, LSD method was used for appropriate pairwise comparisons among treatment groups. Additionally, Dunn's post-hoc test was used for pairwise comparisons of treatment groups. Unless otherwise specified, data are presented as mean ± SD, and $p < 0.05$ was considered statistically significant.

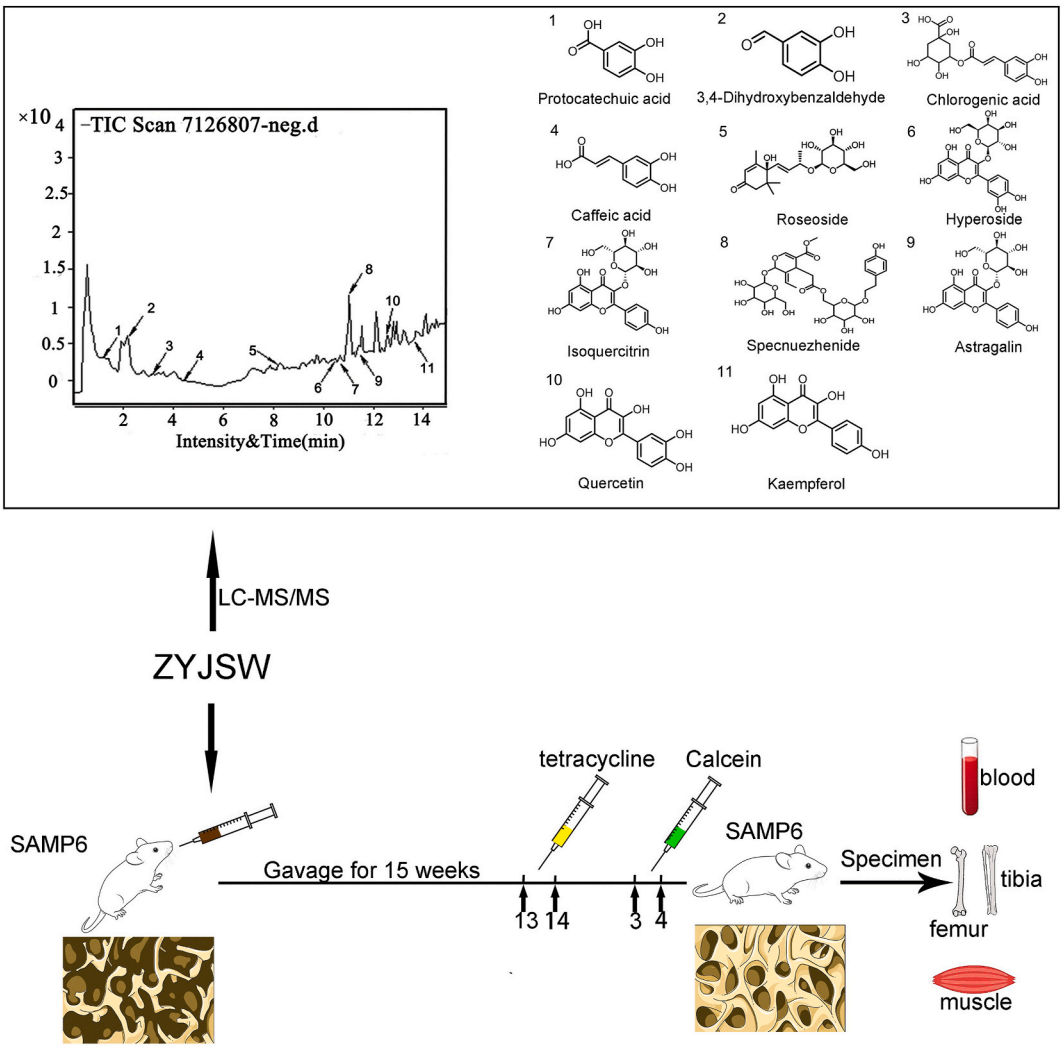

Figure 1. Experimental design flowchart. ZYJSW was administered through gavage for fifteen weeks. Tetracycline was injected subcutaneousionsly in the neck on days 13 and 14 before the experimental end, followed by calcitriol injected as the same manner on days 3 and 4 before the experimental end. Samples of blood, femur, tibia, and muscle were collected for further measurements after sacirfice of mice. Note: ZYJSW refers to Zhuangyao Jianshen Wan; 1–11 represent protocatechuic acid, 3, 4-dihydroxybenzaldehyde, chlorogenic acid, caffeic acid, roseoside, hyperoside, isoquercitrin, specnuezhenide, astragalin, quercetin, and kaempferol, respectively. P6 = SAMP6 mice.

3. Results

3.1. Impact of ZYJSW on organ functions in SAMP6 mice

All mice were orally administered the test substance as the designed plan (Fig. 1). Compared to R1 mice, P6 mice showed a rapid increase in body weight after the 26th week, stabilizing after the 28th week. In comparison to P6 mice, the P6+H and P6+Met groups exhibited smaller fluctuations in average body weight, with the P6+Met group showing lower body weight than the other treatment groups after the 23rd week. After the 28th week, mice in all groups showed a slow increase in body weight, eventually stabilizing, with R1 mice maintaining the lowest weight throughout (Supplementary Fig. 1A). The functions of the spleen, liver and kidney in all seven groups were within the physiological range. H&E staining of the liver showed intact structure, with normal levels of AST and ALT in serum (Supplementary Figs. 2A–C). In the kidneys, SAMP6 mice displayed inflammatory cell infiltration compared to R1 mice, while ZYJSW-treated groups showed no abnormalities (Supplementary Fig. 2C). Despite a significant increase in serum creatinine (Scr) in SAMP6 mice compared to R1 mice, the treatment groups exhibited decreased levels, indicating a protective effect of ZYJSW on SAMP6 mice kidneys (Supplementary Fig. 2B). Overall, ZYJSW did not affect liver and kidney functions in the respective treatment groups.

3.2. ZYJSW improves bone loss and bone quality in SAMP6 mice

In comparison to R1 mice, P6 mice displayed reduced total body bone density and bone mineral content, accompanied by a significant rise in serum β-galactosidase, affirming accelerated aging and bone loss in P6 mice (Fig. 2A and. 3G). Evaluating the protective impact of ZYJSW on bone loss in P6 mice through X-ray measurements of BMD and BMC revealed an increase, indicating its protective effect against bone loss (Fig. 2A). Parameters from the three-point bending test, such as maximum load, fracture load, elastic load, and stiffness coefficient, demonstrated that ZYJSW enhanced the biomechanical performance of bones in P6 mice (Fig. 2B). Microscopy examination of trabeculae structure in P6 mouse femurs indicated that ZYJSW ameliorated trabecular damage (Fig. 2C). Micro-CT scans and 3D reconstruction of trabeculae revealed that compared to the R1 group, the P6 group had fewer trabeculae, some regions within the bone marrow cavity lacked trabeculae, and the trabecular meshwork connecting structure was disrupted. In contrast to the P6 group, mice in the treatment groups showed

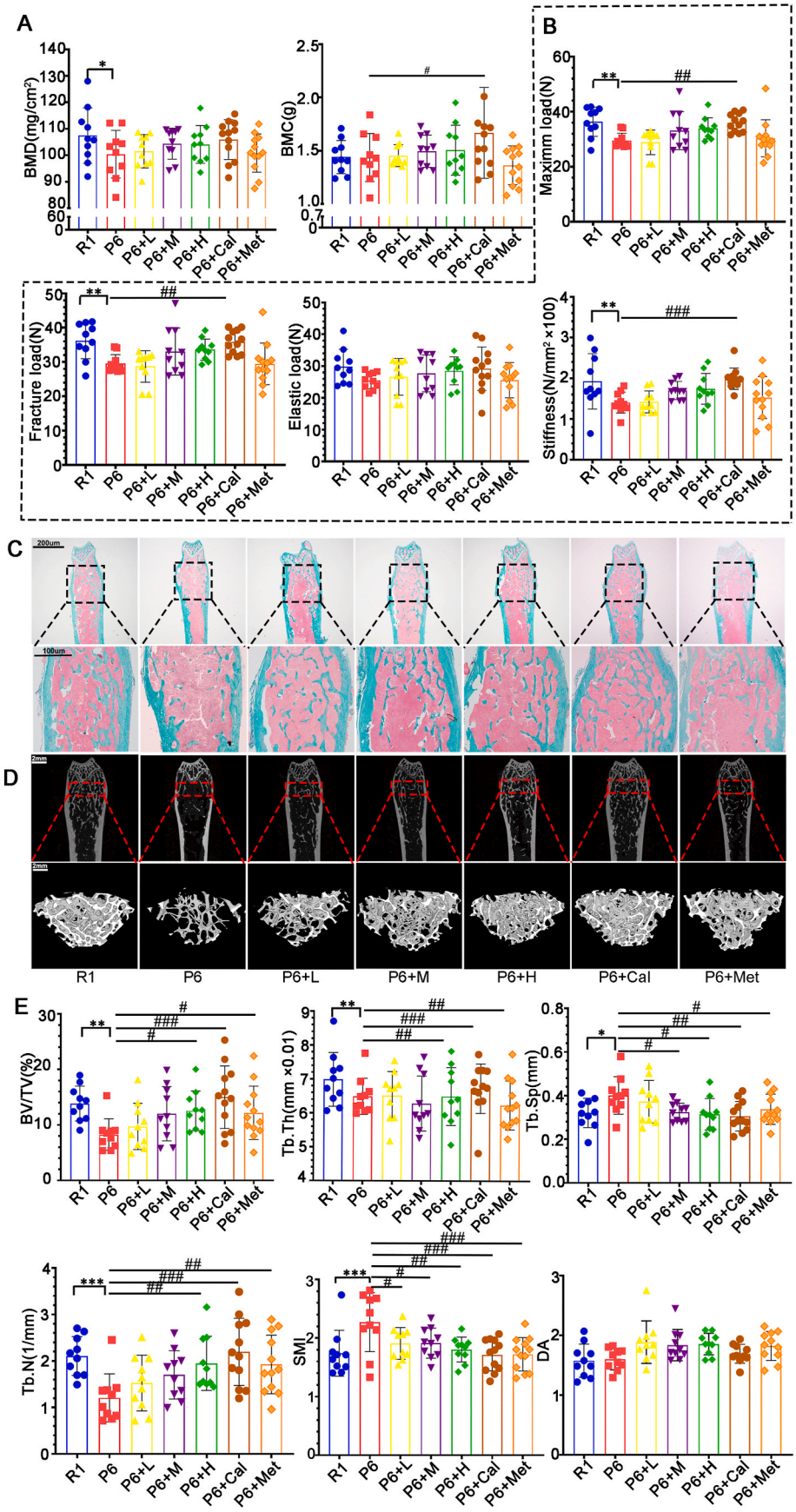

(caption on next page)

Figure 2. Effects of ZYJSW on Bone Mass, Microstructure, and Biomechanical Performance in SAMP6 Mice. (A) BMD and BMC using an X-ray scanner. (B) Results from the three-point bending test, including maximum load, fracture load, elastic load, and stiffness coefficient. (C) Representative images of Goldner staining in the upper segment of the femur. (D) Micro-CT detection of representative 2D and 3D reconstructed images of the distal femur. (E) Quantitative analysis of bone volume fraction (BV/TV), trabecular number (Tb.N), trabecular thickness (Tb.Th), trabecular separation (Tb.Sp), trabecular number (Tb.N), structure model index (SMI), and degree of anisotropy (DA). Data are presented as mean ± SD (n = 10). *$p < 0.05$, **$p < 0.01$, ***$p < 0.001$ vs R1; #$p < 0.05$, ##$p < 0.01$, ###$p < 0.001$ vs P6. Note: The blue box indicates the enlarged area, and the red box represents the 3D reconstruction region. R1=SAMR1 mice; P6=SAMP6 mice; P6+L=SAMP6 mice + low-dose ZYJSW; P6+M=SAMP6 mice + medium-dose ZYJSW; P6+H=SAMP6 mice + high-dose ZYJSW; P6+Cal = SAMP6 mice + calcitriol; P6+Met = SAMP6 mice + metformin. (For interpretation of the references to color in this figure legend, the reader is referred to the Web version of this article.)

an increase in trabecular number, partial restoration of the meshwork structure, with the P6+H and P6+Cal groups showing better restoration of trabecular structure. This further confirms the protective effect of ZYJSW on the bone microstructure of P6 mice, consistent with the BV/TV, Tb.Th, Tb.Sp, Tb.N, SMI, and DA data in the CT reconstruction (Fig. 2D and E). In summary, ZYJSW contributes to increased bone mass and improved bone quality in P6 mice, showing promise for preventing age-related osteoporosis.

3.3. ZYJSW modulates bone metabolism imbalance in SAMP6 mice

Regulating bone remodeling is essential for maintaining the integrity and normal function of the skeletal structure. We explored the potential of ZYJSW to enhance bone metabolism in P6 mice. Using double fluorescence labeling with tetracycline and calcein in the cortical and trabecular bone of the tibia, the results showed that compared to the R1 group mice, the P6 group mice had narrower fluorescent intervals. After administration, there was a recovery in all groups, with the P6+H group and P6+Cal group showing larger fluorescent intervals (Fig. 3A, B, D). Additionally, the trabecular bone at the proximal end of the tibia in all treatment groups showed an increased area occupied by trabecular bone, with a more uniform distribution of trabecular bone (Fig. 3C–E). At the cellular level, Compared to mice in the R1 group, those in the P6 group showed a significant decrease in osteoblasts and an increase in the number and activity of osteoclasts. Treatment with ZYJSW increased the number of osteoblasts, decreased the number of osteoclasts, and inhibited their bone resorption activity (Supplementary Figs. 3A and B). From a serum perspective, ZYJSW decreased the level of the bone resorption marker CTX-I and increased the content of the bone formation marker PINP (Fig. 3F). Overall, ZYJSW can regulate the number and activity of osteoblasts and osteoclasts, promote bone formation, and inhibit bone resorption, thereby improving bone metabolism in P6 mice. This indicates its potential as a therapeutic agent for age-related osteoporosis.

3.4. ZYJSW and SOP network pharmacology analysis

Expanding on ZYJSW's positive influence on bone structure and metabolism in P6 mice, our goal was to identify its active ingredients for age-related osteoporosis treatment. Utilizing LC-MS, we pinpointed 11 potential compounds (Fig. 1). Assessing the complex chemical activity of ZYJSW, consisting of 11 traditional Chinese medicinal herbs, involved predicting and screening 67 active compounds and 310 potential targets. Integration with 1123 targets from TCMSP, SwissTargetPrediction, and PharmMapper associated with age-related osteoporosis yielded 137 potential targets (Fig. 4A). We constructed a protein–protein interaction (PPI) network and identified the top 17 key genes based on their degree values. In this network, AKT1 emerged as a crucial target (Fig. 4B and C). Pathway analysis highlighted the involvement of PI3K/Akt and Wnt signaling pathways (Fig. 4D). Additionally, GO enrichment shows that ZYJSW is associated with myoblast differentiation and mitochondrial regulation (Fig. 4E).

3.5. Molecular docking results

Based on the degree values, we selected the top six small molecular compounds from ZYJSW, which are quercetin, kaempferol, beta-sitosterol, Augelicin, luteolin, and stigmasterol. According to the PPI network, the top four key targets are AKT1, TNF, IL-6, and TP53. Molecular docking was performed for each compound against these targets, and the results were visualized using a heatmap (Fig. 4G). Among them, beta-sitosterol and stigmasterol showed binding energies less than −5 kcal/mol with each target, indicating good binding performance. Therefore, beta-sitosterol and stigmasterol may be important effective components of ZYJSW (Fig. 4F and G). Additionally, all small molecular compounds showed good binding abilities with AKT1, suggesting that AKT1 may be a key target for ZYJSW in treating SOP.

3.6. Proteomic Results of P6 mice and R1 mice

To gain deeper insights into the causes of osteoporosis in P6 mice, we conducted proteomic analysis on the bones of both R1 and P6 mice. The analysis of P6 mice bones identified 188 upregulated genes and 78 downregulated genes. Notably, 31 differentially expressed genes were found in mitochondria (Fig. 5A and B). Subsequent analysis revealed that these differentially expressed genes were associated with 291 pathways, with the PI3K/Akt signaling pathway and Wnt signaling pathway prominently featured among those relevant to osteoporosis (Fig. 5C). Concurrently, GO analysis highlighted a close association between differentially expressed genes and mitochondrial and muscle tissues (Fig. 5D).

The combination of network pharmacology and proteomics provided crucial insights. Firstly, beyond osteoporosis, P6 mice may be vulnerable to muscle-related diseases. Secondly, mitochondria play a crucial role in both the onset and treatment of osteoporosis in P6 mice. Lastly, ZYJSW may enhance osteoporosis in P6 mice through the PI3K/Akt/Wnt signaling pathways.

3.7. Protective effects of ZYJSW on muscle structure and function in SAMP6 mice

Our investigation into P6 mice revealed potential muscle-related diseases, prompting an exploration of ZYJSW's impact on muscle conditions. Through H&E analysis, we observed larger and disorganized muscle cell interspaces in P6 mice compared to R1 mice, indicative of structural disarray (Fig. 6A). However, treatment groups exhibited improved structural abnormalities, demonstrating ZYJSW's muscle-restoring effect. Further assessments on muscle function revealed a significant decrease in Ca^{2+}-Mg^{2+}-ATP and Na^{+}-K^{+}-ATP enzyme activities in P6 mice, with treatment groups showing a substantial increase, particularly in the medium and high-dose categories (Fig. 6B). Additionally, the protein levels of Ub, Murf-1, FBOX32, and Myog in the muscles of P6 mice exhibited significant elevation compared to R1 mice (Fig. 6C, D, E, Supplementary Fig. 5). Nevertheless, in the treatment groups, the expression of these proteins displayed a decreasing trend. These findings suggest abnormal muscle function in P6 mice, with ZYJSW playing a role in restoring it. In summary, P6 mice exhibit evident structural and functional muscle damage, and ZYJSW demonstrates a protective effect on muscle structure and function in this context.

In muscle tissue, ATPase is a marker of fast-twitch muscle fibers and can enhance muscle contraction speed [25]. Additionally, Myostatin is an important negative regulator that inhibits muscle growth and exacerbates muscle mass reduction [26]. Our immunohistochemical analysis

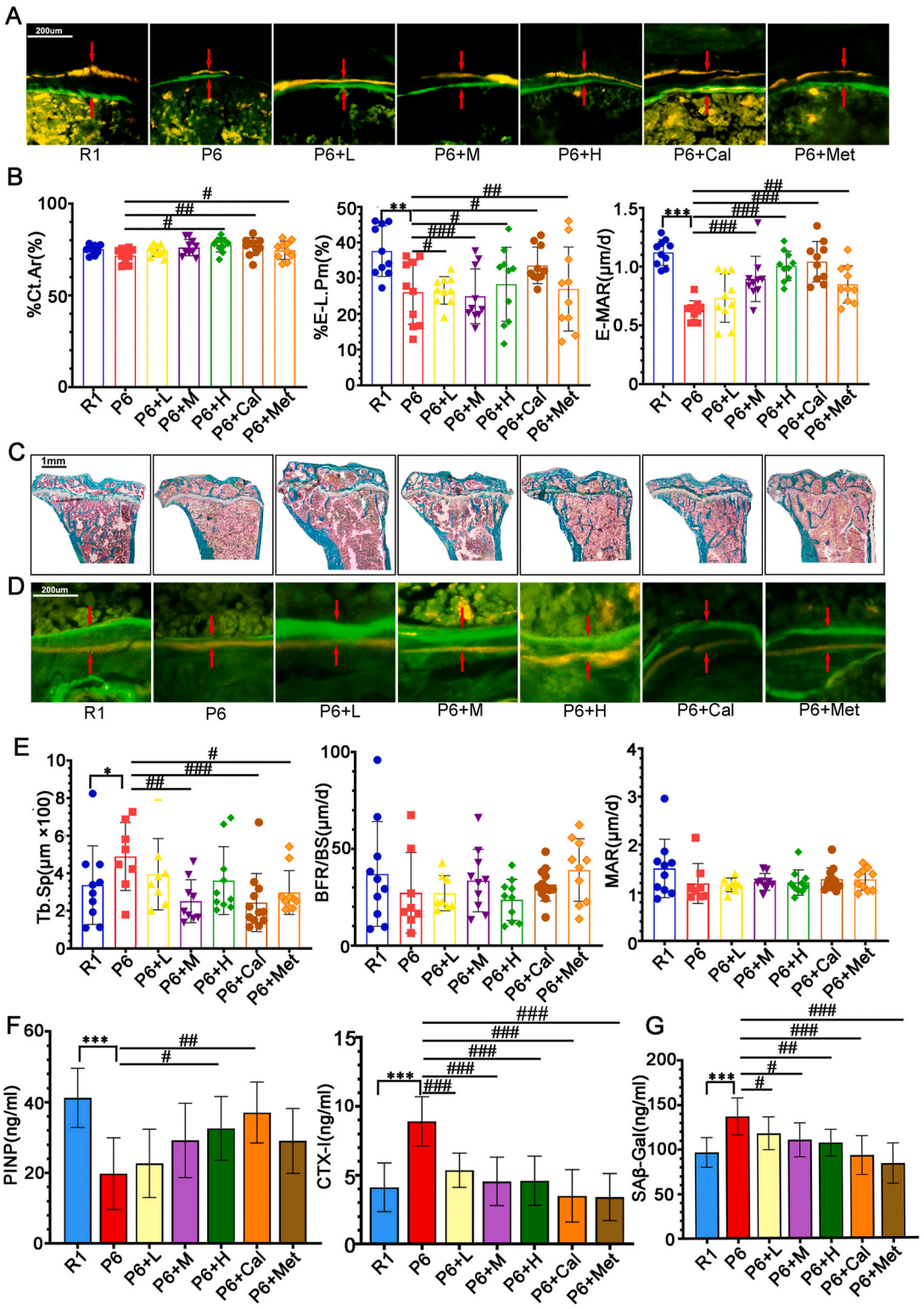

Figure 3. Effects of ZYJSW on Bone Metabolism in SAMP6 Mice. (A) Representative fluorescence microscopy images of tetracycline and calcein double-labeled cortical bone in the midshaft of the tibia. (B) Cortical bone area percentage (Ct.Ar), endocortical labeled perimeter percentage (%E-L.Pm), and endocortical mineral apposition rate (E-MAR). (C) Goldner staining of trabecular bone at the proximal end of the tibia. (D) Representative fluorescence microscopy images of tetracycline and calcein double-labeled trabecular bone at the proximal end of the tibia. (E) Trabecular bone separation (Tb.Sp), bone formation rate per bone surface (BFR/BS), and mineralization apposition rate (MAR) at the proximal end of the tibia. (F) ELISA assay for serum bone formation marker (PINP) and bone resorption marker (CTX-I). (G) Content of β-galactosidase (SAβ-Gal) in serum. Data are presented as mean ± SD (n = 10).*$p < 0.05$, **$p < 0.01$, ***$p < 0.001$ vs R1; #$p < 0.05$, ##$p < 0.01$, ###$p < 0.001$ vs P6.Note: Red arrows indicate double fluorescence. R1 = SAMR1 mice; P6 = SAMP6 mice; P6+L = SAMP6 mice + low-dose ZYJSW; P6+M = SAMP6 mice + medium-dose ZYJSW; P6+H = SAMP6 mice + high-dose ZYJSW; P6+Cal = SAMP6 mice + calcitriol; P6+Met = SAMP6 mice + metformin. (For interpretation of the references to colorin this figure legend, the reader is referred to the Web version of this article.)

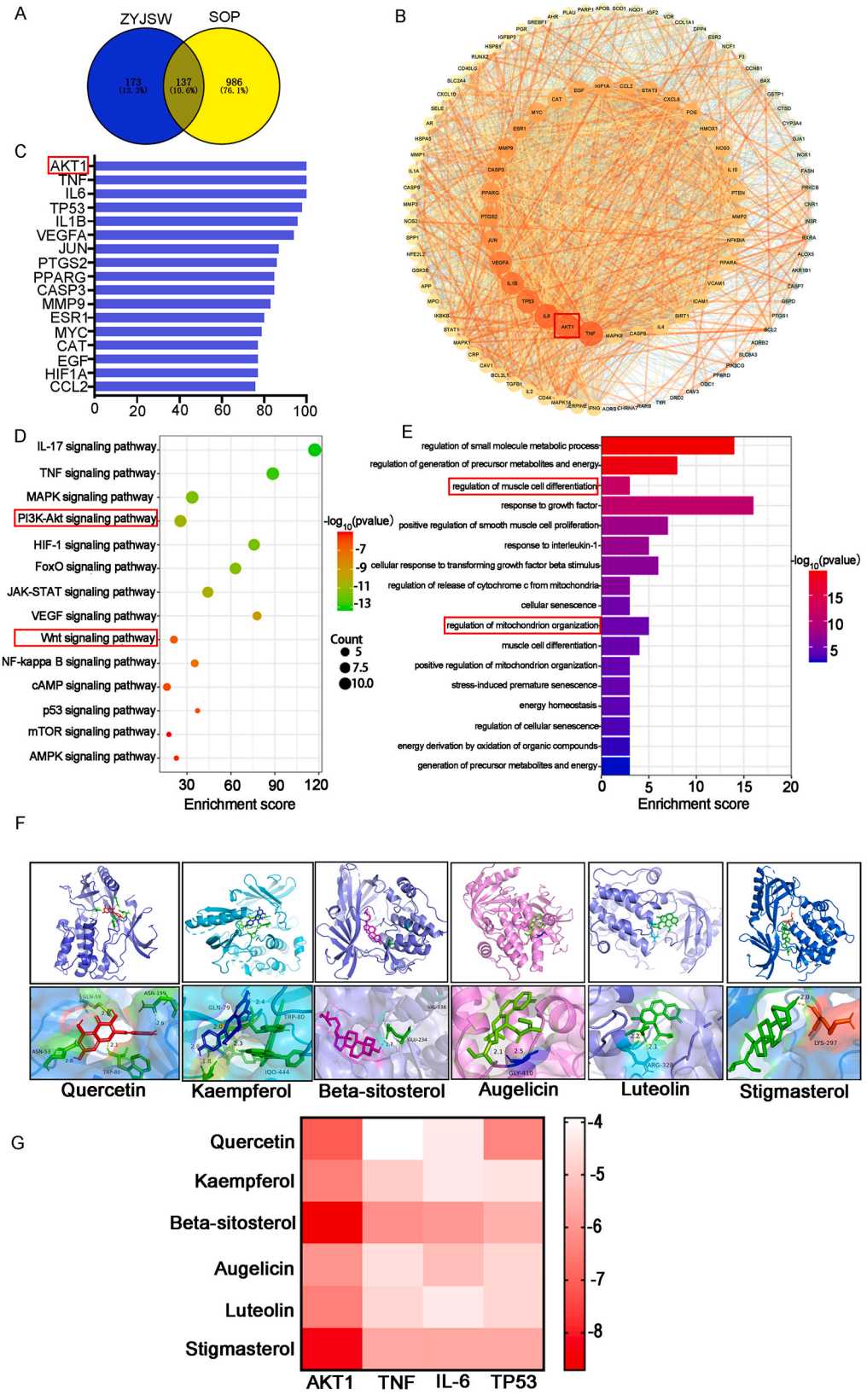

Figure 4. Prediction of Active Ingredients and Targets of in Treating Osteoporosis in SAMP6 Mice. (A) Venn Analysis of Potential Targets Overlapping Between ZYJSW and SOP. (B) Top-Ranked Core Targets:The red box indicates the target with the highest degree value. (C) Network of PPI between Targets of ZYJSW and SOP: The red box indicates the target with the highest degree value. (D) KEGG Enrichment Bubble Chart of Signaling Pathways:The red box highlights pathways associated with osteoporosis. (E) GO Biological Process Enrichment Analysis:The red box highlights processes related to muscle and mitochondria. (F) Docking results of small molecule compounds with protein AKT1. (G)Heat map of the docking energy. Note: R1 = SAMR1 mice; SAMP6 = SAMP6 mice; SAMP6+L = SAMP6 mice + low-dose ZYJSW; SAMP6+M = SAMP6 mice + medium-dose ZYJSW; SAMP6+H = SAMP6 mice + high-dose ZYJSW; SAMP6+Cal = SAMP6 mice + calcitriol; SAMP6+Met = SAMP6 mice + metformin. (For interpretation of the references to color in this figure legend, the reader is referred to the Web version of this article.)

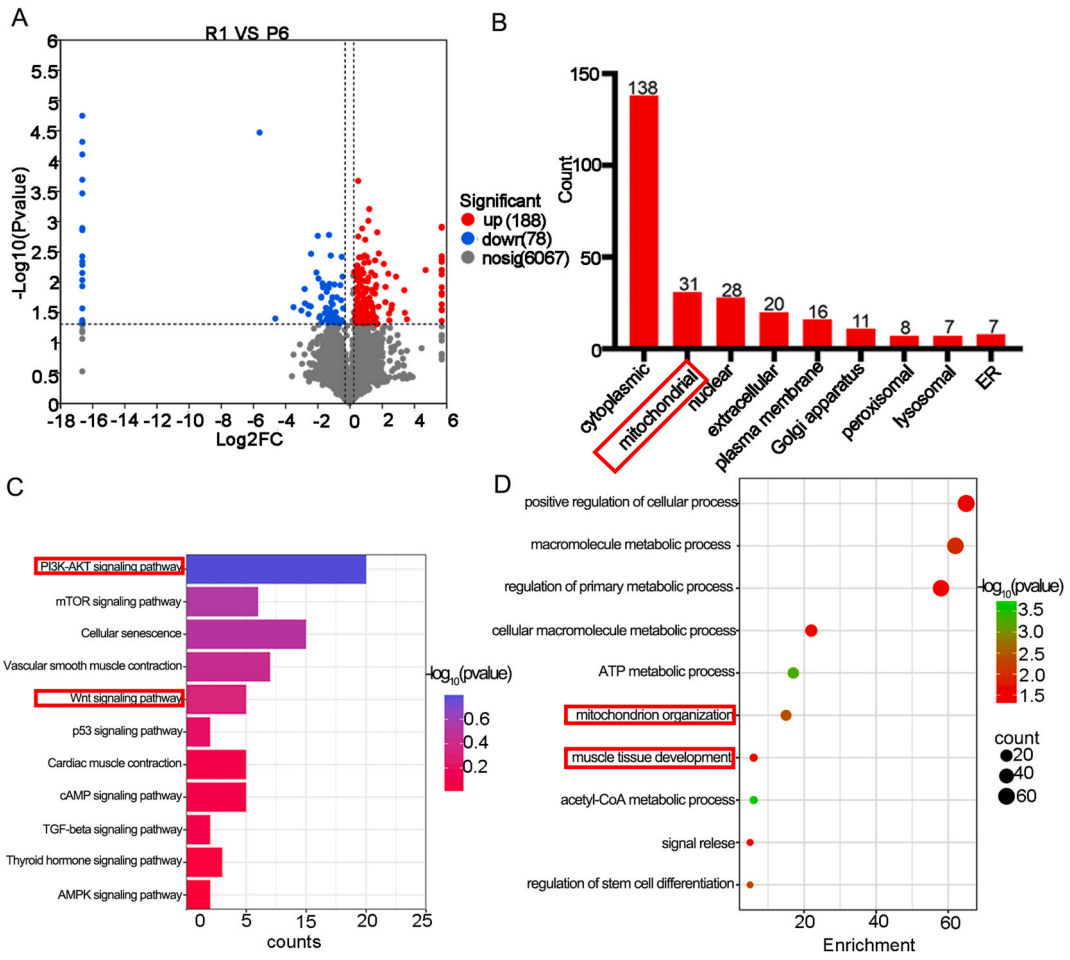

Figure 5. Proteomic Results of P6 Mice and R1 Mice. (A) Volcano Plot of Differentially Expressed Genes (DEGs) between R1 and SAMP6 Mice. (B) Subcellular Localization of DEGs:The red box indicates localization in mitochondria. (C) KEGG Enrichment Bubble Chart of Signaling Pathways for DEGs:The red box highlights pathways associated with osteoporosis. (D) GO Biological Process Enrichment Analysis for DEGs:The red box highlights processes related to muscle and mitochondria. (For interpretation of the references to color in this figure legend, the reader is referred to the Web version of this article.)

of muscle tissue revealed that compared to R1 mice, P6 mice exhibited reduced ATPase expression and increased myostatin expression, reflecting changes in muscle mass and fiber type, with P6 mice developing sarcopenia (Fig. 6F and G). Compared to P6 mice, the various ZYJSW treatment groups showed improvement. To explore the specific mechanism of ZYJSW's effect on sarcopenia, we found that in muscle tissue, compared to R1 mice, P6 mice had increased GCN5L1 expression and decreased β-catenin expression, which was reversed in the ZYJSW treatment groups (Fig. 6F and G). Therefore, we hypothesize that ZYJSW ameliorates sarcopenia in P6 mice by regulating the GCN5L1/Wnt signaling pathway.

3.8. Modulate of P13K/Akt and Wnt Signaling Pathways by ZYJSW

Based on the results from network pharmacology and proteomics, it is evident that the PI3K/Akt and Wnt signaling pathways play crucial roles in the onset and treatment of osteoporosis in P6 mice. Our study found that ZYJSW attenuated the imbalance in bone metabolism by promoting bone formation, as evidenced by the upregulation of key factors such as RUNX2, BMP2, OPG, and OCN, while simultaneously inhibiting bone resorption through the downregulation of TRAF6, TRAP, RANKL, and CTSK (Fig. 7A–F, Supplementary Fig. 4). To explore whether ZYJSW attenuated the imbalance in bone metabolism in P6 mice by modulating the PI3K/Akt and Wnt signaling pathways, we conducted Western blot experiments. The findings revealed that in the ZYJSW treatment group, the expressions of p-PI3K and p-AKT were decreased, suggesting that ZYJSW inhibits PI3K/Akt signaling pathways (Fig. 8A and B). In addition, LRP5, p-GSK-3β, and β-catenin were significantly increased, indicating that Wnt signaling pathways were activated by ZYJSW in P6 mice (Fig. 8C and D). Overall, ZYJSW modulates the PI3K/Akt and Wnt signaling pathways to enhance the balance of bone metabolism in the treatment of SOP in P6 mice.

3.9. Regulation of P13K/Akt and Wnt Signaling Pathways by ZYJSW through GCN5L1

Research indicates that mitochondria may play a role in the development and treatment of osteoporosis in P6 mice. GCN5L1, associated with mitochondrial biogenesis, potentially contributes to its anti-aging effect. To explore the relationship between ZYJSW, GCN5L1, and the PI3K/Akt and Wnt signaling pathways, Western blot experiments were conducted, revealing GCN5L1's involvement in activating the PI3K/Akt signaling pathway through promoting AKT phosphorylation expression (Fig. 8A and B, and Supplementary Fig. 5). Additionally, GCN5L1 indirectly regulates GSK-3β, participating in the Wnt signaling pathway (Fig. 8C and D, and Supplementary Fig. 5). Simultaneously, GCN5L1 regulates β-catenin protein expression by inhibiting mitochondrial biosynthesis proteins PGC-1α, NRF-1, and TFAM and engages in the Wnt signaling pathway (Fig. 8E–G, and Supplementary Fig. 4). In conclusion, GCN5L1, closely correlated with the PI3K/Akt and Wnt signaling pathways, may serve as a potential target for treating SOP. From the above study, we have established that ZYJSW directly or indirectly

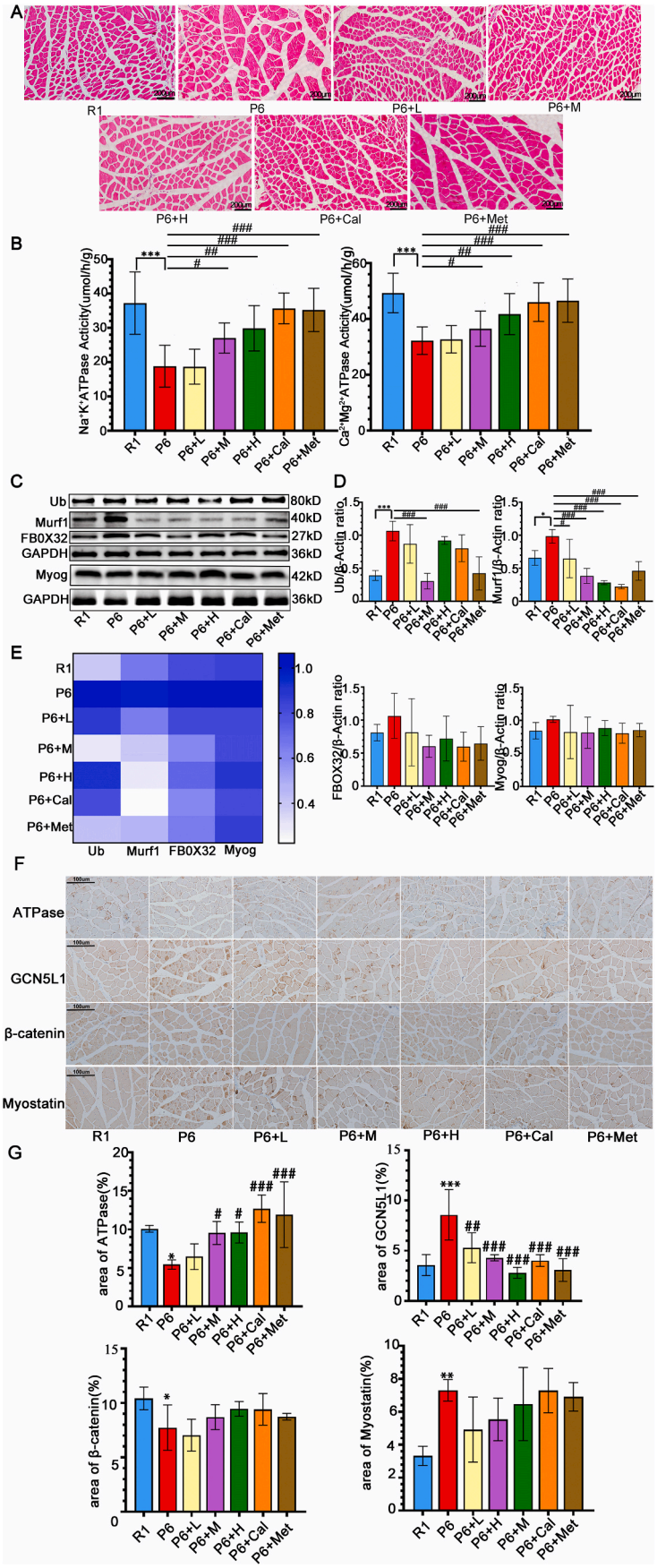

(caption on next page)

Figure 6. Protective Effects of ZYJSW on Muscle Structure and Function. (A) Representative Histopathological Sections of Quadriceps Muscle by H&E Staining (The representative images illustrate the protective effects of ZYJSW on muscle structure). (B) Activity of Na^+-K^+-ATPase and Ca^{2+}-Mg^{2+}-ATPase in Quadriceps Muscle: The activities of Na^+-K^+-ATPase and Ca^{2+}-Mg^{2+}-ATPase in the quadriceps muscle were measured to evaluate muscle function. (C) Protein Expression Levels of Ubiquitin (Ub), Murf-1, FBOX32, and Myogenin (Myog) by Western Blot: Western blot analysis was performed to determine the protein expression levels of Ub, Murf-1, FBOX32, and Myog in the quadriceps muscle. Representative images are shown. (D) Quantification of Ub, Murf-1, FBOXO32, and Myog: Quantitative analysis of Ub, Murf-1, FBOX32, and Myog protein expression levels based on three independent experiments. (E) Heatmap Analysis of Ub, Murf-1, FBOX32, and Myog Protein Expression:A heatmap representation was generated to visualize the protein expression levels of Ub, Murf-1, FBOX32, and Myog, averaged from three independent experiments. (F) Representative images of immunohistochemistry. (G) Percentage of the area of positive regions in immunohistochemistry. $^*p < 0.05$, $^{**}p < 0.001$ vs R1; $^{\#}p < 0.05$, $^{\#\#}p < 0.01$, $^{\#\#\#}p < 0.001$ vs P6. Note: R1=SAMR1 mice; P6=SAMP6 mice; P6+L=SAMP6 mice + low-dose ZYJSW; P6+M=SAMP6 mice + medium-dose ZYJSW; P6+H=SAMP6 mice + high-dose ZYJSW; P6+Cal = SAMP6 mice + calcitriol; P6+Met = SAMP6 mice + metformin.

involves PI3K/Akt through the inhibition of GCN5L1 expression, revealing its potential mechanism in treating SOP.

4. Discussion

Currently, there is a global urgency to develop new drugs with low toxicity and high efficacy for SOP due to the rising elderly population [27]. ZYJSW, a canonical prescription of TCM, presents a promising avenue for exploring its potential in the healing of osteoporotic lumbar compression fractures in the elderly [28]. Our present study highlights the intervening effect of ZYJSW on SOP. More precisely, it elucidates the preventive efficacy of ZYJSW in inhibiting bone loss, leading to impaired microarchitecture and ultimately diminished bone quality in P6 mice. The study results found that ZYJSW most significantly improved the microarchitecture of trabecular bone in cancellous bone. It also improved bone biomechanical properties, though the effect was not significant. The percentage of cortical bone area (%Ct.Ar) showed little change across the groups, suggesting that ZYJSW has a better effect on improving cancellous bone while having a smaller impact on cortical bone.Through network pharmacology, proteomics, and literature research, we propose GCN5L1 as a potential target for ZYJSW in treating SOP. In the skeletal pathological condition associated with aging, GCN5L1 may induce downregulation of the Wnt signaling by activating PI3K/Akt pathways and simultaneously inhibiting mitochondrial biogenesis. Consequently, osteoblast differentiation, responsible for bone formation, is inhibited during the pathological process of SOP (Fig. 9). The predicted mechanism was validated through *in vivo* measurement of the relevant pathways using Western blotting assays. Consequently, ZYJSW holds significant promise as an active candidate for further research and development of SOP.

In animal experiments, the selection of positive control drugs is crucial as they serve not only as a benchmark for therapeutic efficacy but also ensure the scientific rigor and reliability of the experimental design and results. Moreover, they provide a direct comparative standard for new drugs or treatment methods. 1, 25-Dihydroxyvitamin D3 (active vitamin D3) is an FDA-approved drug for treating osteoporosis and other bone-related diseases [29]. It enhances the absorption of calcium and phosphorus in the intestines and directly stimulates the activity of osteoblasts. Numerous studies have shown that 1, 25-dihydroxyvitamin D3 can increase BMD and reduce the risk of fractures in osteoporosis patients, demonstrating good efficacy in postmenopausal women and elderly men [30]. Due to its mechanism of action in bone protection, it is often chosen as a positive control drug in anti-osteoporosis treatment studies. Metformin is a commonly used oral hypoglycemic drug mainly used to treat type 2 diabetes. Recent studies have found that metformin has a significant bone-protective effect [31]. Clinical studies have shown that diabetic patients taking metformin have higher bone density and lower fracture risk. Additionally, metformin has shown positive effects in anti-aging research, prolonging lifespan, improving health status, and inhibiting cell aging. Therefore, metformin is often selected as a positive drug in anti-aging research [32]. This study selected 1,25-dihydroxyvitamin D3 as the positive drug for evaluating bone protection and metformin as the positive drug for evaluating anti-aging effects, in order to investigate in depth their mechanisms of action and clinical applications in osteoporosis and aging-related diseases.

The careful selection of animal models is essential in the study of pharmacological agents for SOP, as the selected model needs to faithfully represent the skeletal changes occurring during the aging process. At present, there are three types of animal models for SOP: natural aging SOP, D-galactose-induced SOP, and rapid aging SOP (such as P6 mouse). In the natural aging SOP model, which mimics human aging changes of bone tissues under normal conditions, challenges arise with a cultivation period exceeding 12 months and associated high expenses [33]. D-galactose aging models involve daily administration, offering simplicity but facing challenges in maintaining consistent drug delivery and stability [33]. Rapid aging models, like the P6 mouse, present a variety of strains resembling human age-related osteoporosis. Despite aging occurring spontaneously, SAM mice demonstrate genetic stability, making them a suitable choice considering experimental need. In P6 mouse, the clinical signs, pathological traits, and pathogenesis closely mimic human SOP, rendering it an ideal model for SOP research [23]. Previous evidence has shown that peak BMD in 4–5 month old P6 mice, followed by a rapid decline, aligns with age-dependent BMD changes observed in the elderly [34]. Therefore, we chose 4-month-old P6 mice to establish an experimental model of SOP. Generally, data acquisition proves challenging in the SOP model as bone loss is irreversible, and excessive bone loss does not adequately capture the effectiveness of pharmacological treatments [35,36]. Hence, we selected the 15-week gavage period as the experimental endpoint to observe pathological phenotypes, and appraise the intervention effect of ZYJSW on SOP. Notably, we calculated the clinical equivalent dose based on a clinical trial and set the “medium dose” in P6 mice, followed by the “low dose” and “high dose” of ZYJSW, in accordance with specified ratios referenced to the Guide of Preclinic Research [37]. In this study, although the efficacy of ZYJSW from P6 mice was noteworthy, a more detailed understanding of the mechanism requires further investigation using GCN5L1 knockout mice.

Mitochondrial biogenesis involves the generation of new mitochondria through the coordinated regulation of mitochondrial DNA (mtDNA) and nuclear DNA (nDNA), ensuring normal mitochondrial function in bone tissues [38]. PGC-1α, a major regulator of mitochondrial biogenesis, can facilitate the differentiation of bone marrow-derived mesenchymal stem cells (BMSCs) into osteoblasts [39]. Under normal physiological conditions, PGC-1α contributes to activating the transcription of NRF-1 and regulating the expression of mitochondrial nuclear-encoded genes (such as TFAM), collectively governing mitochondrial biosynthesis [40]. Our results demonstrate that ZYJSW upregulates the expression of PGC-1α, NRF-1, and TFAM, resulting in an increase in mitochondrial biogenesis in P6 mice. Strikingly, GCN5L1, a protein linked to mitochondrial biosynthesis, reveal a progressive increase of its expression with aging in our study, consistent with previous findings [41]. Further investigation is needed to identify specific molecules within the GCN5L1 pathway that are involved in mitochondrial biogenesis, osteoblast proliferation, and differentiation. These evidences suggest that GCN5L1 has potential as a target for SOP treatment.

Distinctively, GCN5L1 is closely linked to the PI3K/Akt and Wnt signaling pathways [11,42]. In our study, GCN5L1 expression was supprssed in P6 mice exposed to ZYJSW, potentially contributing to its anti-aging effect. The decrease in Akt and GSK-3β phosphorylation after GCN5L1 knockdown further highlights the critical involvement of

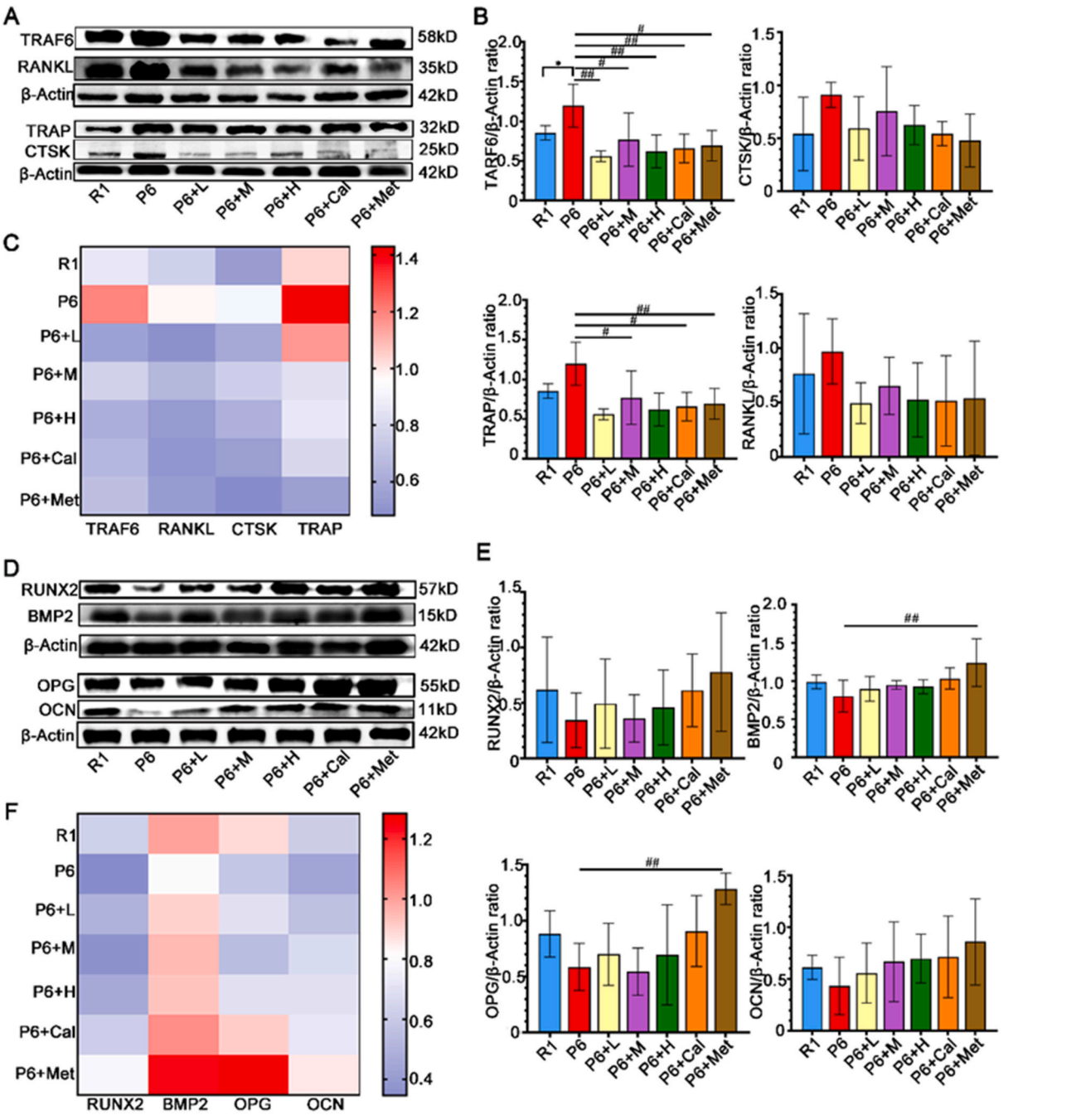

Figure 7. Effects of ZYJSW on Bone-Related Proteins in Bone Formation and Resorption. (A) Representative images of protein bands for TRAF6, TRAP, RANKL, and CTSK involved in bone resorption (The representative images shown are from one independent experiment out of three repeated experiments). (B) Quantification of TRAF6, TRAP, RANKL, and CTSK proteins (Data represent mean ± SD of three independent experiments). (C) Heatmap analysis of TRAF6, TRAP, RANKL, and CTSK protein expressions (Plotted using the average values from three experiments). (D) Representative images of protein bands for RUNX2, BMP2, OPG, and OCN involved in bone formation (The representative images shown are from one independent experiment out of three repeated experiments). (E) Quantification of RUNX2, BMP2, OPG, and OCN proteins (Data represent mean ± SD of three independent experiments). (F) Heatmap analysis of RUNX2, BMP2, OPG, and OCN protein expressions (Plotted using the average values from three experiments). *$p < 0.05$ vs R1; #$p < 0.05$, ##$p < 0.01$ vs P6. Note: R1=SAMR1 mice; P6=SAMP6 mice; P6+L=SAMP6 mice + low-dose ZYJSW; P6+M=SAMP6 mice + medium-dose ZYJSW; P6+H=SAMP6 mice + high-dose ZYJSW; P6+Cal = SAMP6 mice + Calcitriol; P6+Met = SAMP6 mice + Metformin.

GCN5L1 in regulating PI3K/AKT/Wnt pathways [13]. Our research also found that decreased GCN5L1 expression was accompanied by decreased of phosphorylation both PI3K and Akt, simutanious increase of GSK3-β phosphorylation in the P6 mice treated with ZYJSW. Given that GSK-3β plays a pivotal role in the regulation of the Wnt signaling pathway, a classical pathway in regulating osteoblast differentiation, the relationship between GCN5L1 and Wnt is considerable interest in further study. Genuinely, deletion of GCN5L1 has been shown to induce the expression of PGC-1α, thereby initiating mitochondrial biogenesis [10]. Parallelly, PGC-1α knockdown results in decrease in GSK-3 (ser9) phosphorylation, followed by the reduced expression of β-catenin [43], suggesting downregulation of Wnt signaling. Mitochondrial biogenesis plays a vital role in both activation and function of mitochondria. Conversely, mitochondrial function mirrors the potential of

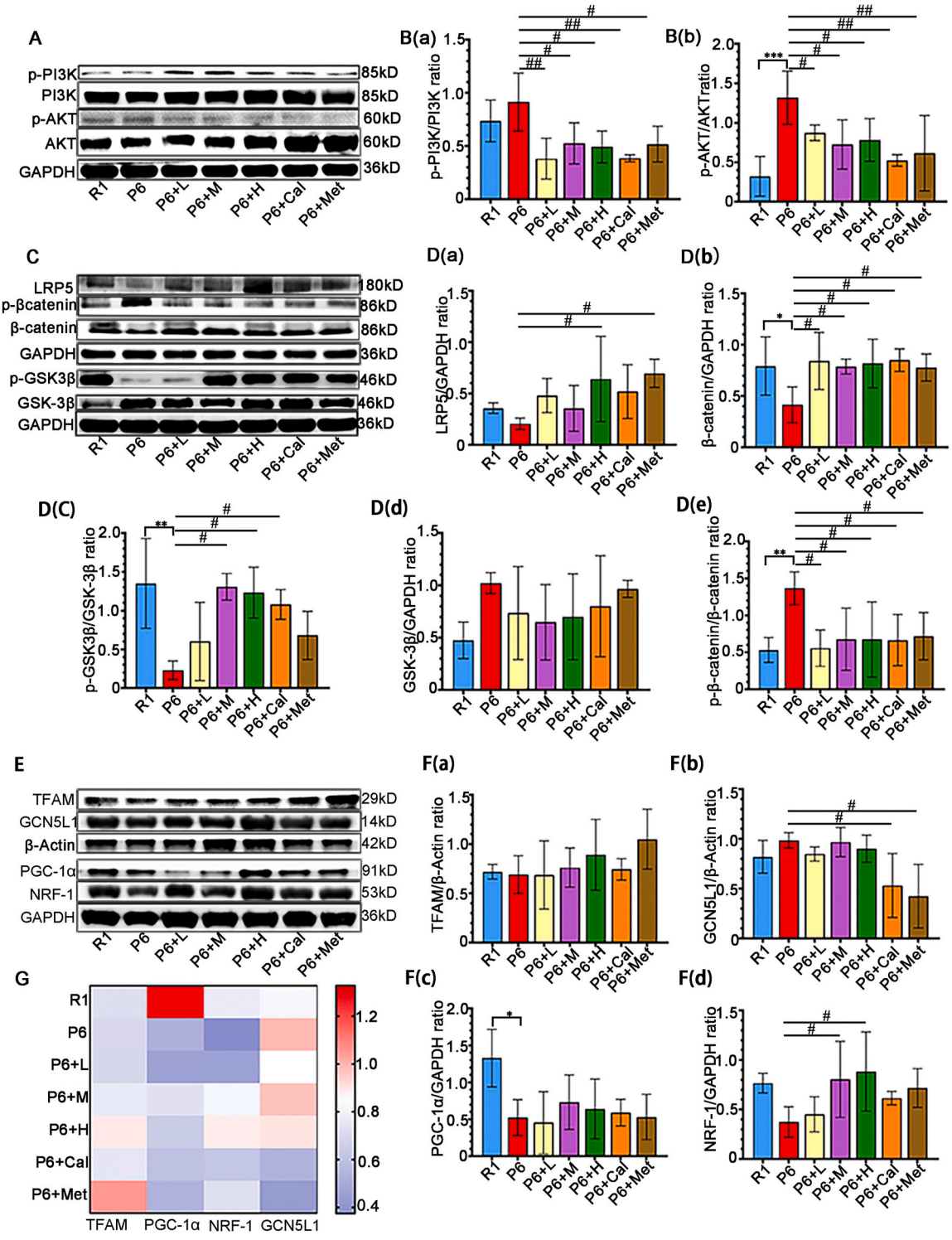

Figure 8. ZYJSW Regulates the P13K/Akt and Wnt Signaling Pathways via GCN5L1. (A) Western blot analysis of P13K/Akt signaling pathway protein expressions (The representative images shown are from one independent experiment out of three repeated experiments). B (a)-B (b) Quantification of protein bands for p-PI3K, p-AKT (Data represent mean ± SD of three independent experiments). (C) Western blot analysis of Wnt pathway protein expressions (The representative images shown are from one independent experiment out of three repeated experiments). D(a)-D(e) Quantification of protein bands for LRP5, β-catenin, GSK-3β, p-β-catenin, and p-GSK-3β (Data represent mean ± SD of three independent experiments). (E) Representative images of protein bands for TFAM, GCN5L1, PGC-1α, NRF-1 involved in mitochondrial biogenesis (The representative images shown are from one independent experiment out of three repeated experiments). F(a)-F(d) Heatmap analysis of TFAM, PGC-1α, NRF-1, GCN5L1 protein expressions (Plotted using the average values from three experiments). (G) Quantification of protein bands for TFAM, GCN5L1, PGC-1α, and NRF-1 (Data represent mean ± SD of three independent experiments). *p < 0.05, **p < 0.01, ***$p < 0.001$ vs R1; $^{\#}p < 0.05$, $^{\#\#}$p < 0.01 vs P6. Note: Red arrows indicate dual fluorescence; R1=SAMR1 mice; P6=SAMP6 mice; P6+L=SAMP6 mice + low-dose ZYJSW; P6+M=SAMP6 mice + medium-dose ZYJSW; P6+H=SAMP6 mice + high-dose ZYJSW; P6+Cal = SAMP6 mice + Calcitriol; P6+Met = SAMP6 mice + Metformin. (For interpretation of the references to color in this figure legend, the reader is referred to the Web version of this article.)

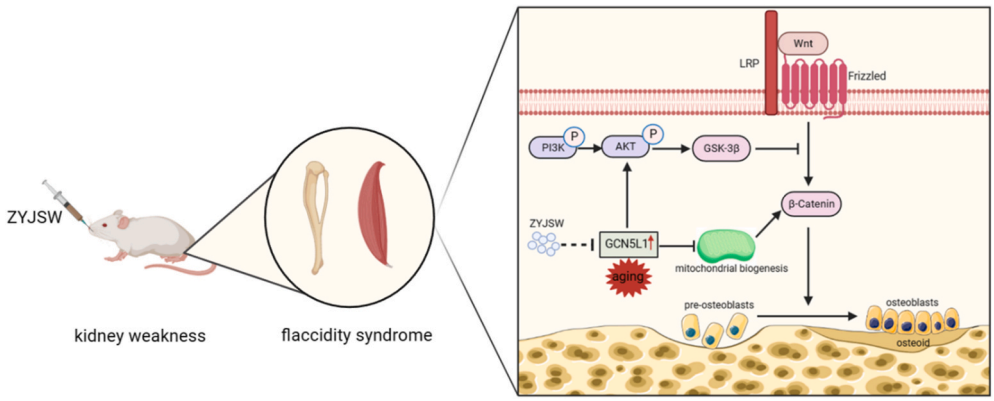

Figure 9. Molecular Mechanism Diagram illustrating the involvement of ZYJSW in Osteoblast Differentiation in SOP.
In the aging process, Kidney Deficiency can lead to the manifestation of symptoms such as osteoporosis and muscle loss, accompanied by an increase in GCN5L1 expression. Subsequently, the PI3K/Akt pathway is activated, directly inhibiting the Wnt/β-catenin pathway, leading to the development of osteoporosis. Meanwhile, GCN5L1 causes a decrease in the expression of proteins related to mitochondrial biogenesis (such as TFAM, PGC-1α, and NRF-1), indirectly affecting the transduction of the Wnt signaling pathway. However, ZYJSW regulates PI3K/Akt and mitochondrial biogenesis through GCN5L1, thereby upregulating the Wnt/β-catenin pathway, ultimately exerting anti-osteoporotic effects and treating Kidney Deficiency syndrome.

mitochondrial biogenesis. Wnt signaling shows a decrease when mitochondrial function is hindered by drugs such as uncouplers and respiratory-chain inhibitors [44], indicating an interconnection between mitochondrial function and the Wnt pathway. Moreover, mitochondrial activation promotes osteogenic differentiation by stimulating β-catenin acetylation [12], further reinforcing this relationship. Based on the aforementioned evidence, we propose that GCN5L1 may restrain the Wnt signaling pathway by diminishing mitochondrial biogenesis. Our results emphasize that a decrease in GCN5L1 expression is accompanied by an increase in protein expressions associated with mitochondrial biogenesis in P6 mice, including TFAM, PGC-1α, NRF-1, as well as elevated β-catenin expression. In a word, GCN5L1 induce a series of molelular events with aging, potentially contributing to downregulation of Wnt signaling in bone tissues. Conversely, ZYJSW may exert preventive effect on SOP by regulating GCN5L1/PI3K/Akt/Wnt pathway.

ZYJSW is extensively employed for its diverse advantages, including strengthening the kidneys, tonifying the waist, dispelling wind, and activating collaterals according to TCM theory. *C. barometz* and *C. chinensis* are designated as Sovereign herbs; *Taxillus Herba*, *L. lucidum*, and *R. laevigata Michx* are categorized as Minister herbs, while, *Spatholobi Caulis*, *Flemingia Roxb*, *K. coccinea*, and *M. speciosa champ* act as adjuvant herbs. Modern investigations highlight that ZYJSW plays a pivotal role in combating oxidative damage by stimulating reduced glutathione generation and reducing malondialdehyde production, demonstrating its antioxidative capabilities, and the subsequent anti-aging effects [45]. Clinically, ZYJSW prescription exhibits effectiveness in managing lumbar vertebral compression fractures in elderly individuals, and while its application on SOP is to be developed due to potential bone-protective properties of its ingredients. Initially, *C. barometz* and *Flemingia Roxb* stimulate bone formation through the promotion of osteoblast differentiation, while *M. speciosa champ* and *spatholobi Caulis* inhibit bone resorption by suppressing osteoclast differentiation [46–49]. Together, these four herbs collectively contribute to the enhancement of bone metabolism in a similar manner. Furthermore, *C. chinensis* modulates miR-21-5p and enhances Fas L protein [50], *Taxilli Herba* counteracts the decrease in E2 levels, and *L. lucidum* promotes the activation of Wnt/β-catenin signaling [51]. Their combined effects contribute uniquely to ameliorating osteoporosis through diverse mechanisms. Besides, *K. coccinea* and *R. laevigata Michx* possessexhibit dual anti-inflammatory and antioxidative properties [52, 53], indicating their potential in osteoporosis treatment, as both inflammation and oxidative stress are significant risk factors for bone health. To sum up, all nine ingredients in the ZYJSW formula play a role in inhibiting osteoporosis, either directly or indirectly. Consequently, the ZYJSW recipe holds substantial potential for the practical treatment of SOP.

Next, ZYJSW exhibits a rich pharmacological profile against SOP in our sdudy, while the specific active ingredients targeting osteoporosis remain unclear. As a result, we identified 11 kinds of compounds using LC-MS/MS analysis, including protocatechuic acid, 3, 4-Dihydroxybenzaldehyde, chlorogenic acid, caffeic acid, roseoside, hyperoside, isoquercitrin, spcnuezhenide astragalin, quercetin and kaempferol. These compounds were used to exploring their preventive effects on osteoporosis except for roseoside. Moreover, quercetin has been shown in numerous studies to regulate the PGC-1α molecule, PI3K/Akt pathway, and Wnt signaling. However, it is a prevalent component found in numerous herbs [54,55]. Additionally, polysaccharide in *R. laevigata Michx* and formononetin sourced from *spatholobi Caulis* exhibit potential in modulating the PI3K/Akt pathway, yet their impact on SOP requires further clarification [53,56]. Additional data on active components and conducting mechanism studies are essential for determining the future effectiveness of ZYJSW in treating SOP.

Research has shown that ZYJSW has a protective effect on the bones of rapidly aging SAMP6 mice, providing an experimental basis for its potential application in the prevention and treatment of SOP. Additionally, the study found that ZYJSW can exert its effects by modulating the PI3K/Akt/Wnt signaling pathway mediated by GCN5L1. This provides a new understanding of the mechanism of action of ZYJSW and also suggests new avenues for developing drugs targeting this signaling pathway. From a clinical perspective, these findings provide a scientific basis for using ZYJSW to treat elderly patients with osteoporosis. ZYJSW may be a potential drug treatment option, especially for patients who cannot tolerate current drug treatments or need alternative treatment options. While the results of animal experiments are encouraging, large-scale randomized controlled clinical trials are still needed to validate the safety and efficacy of ZYJSW in humans. Future research should include patients of different ages, genders, and severity of osteoporosis to comprehensively evaluate the effectiveness of ZYJSW. Further optimization of the dosage and administration of ZYJSW should be conducted to ensure maximum efficacy and minimize side effects in clinical use. Considering our experimental results, a medium dose may be a good choice. Additionally, the effects of combining ZYJSW with other anti-osteoporosis drugs should be studied to explore more effective comprehensive treatment options.

Our study has some limitations that must be acknowledged. Firstly, although we have confirmed that ZYJSW can improve osteoporosis and muscle loss in SAMP6 mice, further research is needed to determine if it can produce the same effects in other SOP animal models. Additionally,

while we primarily focused on the PI3K/Akt/Wnt pathway in our study, ZYJSW's effects on osteoporosis may be related to other pathways as well. Furthermore, while our study provides some evidence supporting a relationship between GCN5L1 and mitochondrial biogenesis, more evidence is needed to confirm this. To further explore the role of GCN5L1 in osteoporosis, it is necessary to conduct in-depth studies using GCN5L1 knockout mice.In summary, our study is the first to demonstrate the inhibitory effects of ZYJSW on osteopenia, muscle loss, impaired bone microstructure, and poor bone and muscle quality, contributing to in treating SOP in P6 mice. Our results also highlight the underlying mechanism that ZYJSW may regulate the PI3K/Akt/wnt signaling pathway by restraining GCN5L1, suggesting that GCN5L1 may be a key target for ZYJSW in the treatment of SOP. This study provides important acknowledges for further exploring the potential of ZYJSW as a new thera-peutic strategy for SOP.

Funding information

The study was supported by National Science Foundation of China, China (Grant Nos. 82274614 and 82174123); Guangdong Basic and Applied Basic Research Foundation, China (Grant No. 2020A1515010058); National Natural Science Foundation of Shenzhen Municipality, China (Grant No. JCYJ20180306174037820); Research Initiation Fund for Doctoral Teachers of Guangdong Medical University, China (Grant No. 2XB17004); Guangdong Province General University Youth Innovative Talent Project, China (2023KQNCX024); Guangdong Medical Science and Technology Research Fund Project, China (A2024186); the Discipline Construction Project of Guangdong Medical University, China (Grant No. 4SG23002G). Nature Science Foundation of Guangdong Province (No. 2022A1515220166, 2023A1515011091), the Science and Technology Foundation of Zhanjiang (No. 2022A01099, 2022A01163, 2022A01170), the Discipline Construction Fund of Central People's Hospital of Zhanjiang (No. 2022A09)

Ethics statement

All animal experiments were approved by Ethics Committee of Guangdong Medical University on Laboratory Animal Care (Resolution number: GDY1902063; Resolution date: Mar 11, 2019).

Authorship & conflicts of interest statement

Authorship

All persons who meet authorship criteria are listed as authors, and all authors certify that they have participated sufficiently in the work to take public responsibility for the content, including participation in the concept, design, analysis, writing, or revision of the manuscript. Each author certifies that this material or part thereof has not been published in another journal, that it is not currently submitted elsewhere, and that it will not be submitted elsewhere until a final decision regarding publication of the manuscript in Journal of Orthopaedic Translation has been made. Conception and design of study: Y.J. Yang, D.T. Wang,Y.Z. Liu. Acquisition of data: S.Y. Ma, J. Lin, M. Yang, J.J. Wang, L.J. Lu, Y. Liang, Y. Yang. Analysis and/or interpretation of data: Y.J.Yang, S.Y. Ma, J. Lin, M.Yang, J.J. Wang. Drafting the manuscript: S.Y. Ma, J. Lin, M.Yang, M. Yang, J.J. Wang revising the manuscript critically for important intellectual content: Y.J.Yang, D.T. Wang, Y.Z. Liu. Approval of the version of the manuscript to be published: S.Y. Ma, J. Lin, M. Yang, J.J. Wang, L.J. Lu, Y. Liang, Y. Yang, Y.J.Yang, D.T. Wang, Y.Z. Liu.

Author names and details of the conflict(s) of interest

This *Authorship & Conflicts of Interest Statement* is signed by all the authors listed in the manuscript to indicate agreement that the above information is true and correct (*a photocopy of this form may be used if there are more than 10 authors*).

Acknowledgements

All persons who have made substantial contributions to the work reported in the manuscript (e.g., technical help, writing and editing assistance, general support), but who do not meet the criteria for authorship, are named in the Acknowledgements and have given us their written permission to be named. If we have not included an Acknowledgements, then that indicates that we have not received substantial contributions from non-authors.

Appendix A. Supplementary data

Supplementary data to this article can be found online at https://doi.org/10.1016/j.jot.2024.08.009.

References

[1] Gregson CL, Armstrong DJ, Bowden J, Cooper C, Edwards J, Gittoes NJL, et al. UK clinical guideline for the prevention and treatment of osteoporosis. Arch Osteoporosis 2022;17(1):58.
[2] Wu D, Li L, Wen Z, Wang G. Romosozumab in osteoporosis: yesterday, today and tomorrow. J Transl Med 2023;21(1):668.
[3] Miller PD. Management of severe osteoporosis. Expet Opin Pharmacother 2016;17(4):473–88.
[4] Lee SY, An HJ, Kim JM, Sung MJ, Kim DK, Kim HK, et al. PINK1 deficiency impairs osteoblast differentiation through aberrant mitochondrial homeostasis. Stem Cell Res Ther 2021;12(1):589.
[5] Jornayvaz FR, Shulman GI. Regulation of mitochondrial biogenesis. Essays Biochem 2010;47:69–84.
[6] Wu K, Scott I, Wang L, Thapa D, Sack MN. The emerging roles of GCN5L1 in mitochondrial and vacuolar organelle biology Biochimica et biophysica acta Gene regulatory mechanisms 2021;1864(2):194598.
[7] Scott I, Wang L, Wu K, Thapa D, Sack MN. GCN5L1/BLOS1 links acetylation, organelle remodeling, and. Metabolism Trends in cell biology 2018;28(5):346–55.
[8] Meng J, Zhang C, Wang D, Zhu L, Wang L. Mitochondrial GCN5L1 regulates cytosolic redox state and hepatic gluconeogenesis via glycerol phosphate shuttle GPD2. Biochem Biophys Res Commun 2022;621:1–7.
[9] Lv T, Zhang Y, Ji X, Sun S, Xu L, Ma W, et al. GCN5L1-mediated TFAM acetylation at K76 participates in mitochondrial biogenesis in acute kidney injury. J Transl Med 2022;20(1):571.
[10] Scott I, Webster BR, Chan CK, Okonkwo JU, Han K, Sack MN. GCN5-like protein 1 (GCN5L1) controls mitochondrial content through coordinated regulation of mitochondrial biogenesis and mitophagy. J Biol Chem 2014;289(5):2864–72.
[11] Donato V, Bonora M, Simoneschi D, Sartini D, Kudo Y, Saraf A, et al. The TDH-GCN5L1-Fbxo15-KBP axis limits mitochondrial biogenesis in mouse embryonic stem cells. Nat Cell Biol 2017;19(4):341–51.
[12] Shares BH, Busch M, White N, Shum L, Eliseev RA. Active mitochondria support osteogenic differentiation by stimulating β-catenin acetylation. J Biol Chem 2018;293(41):16019–27.
[13] Manning JR, Thapa D, Zhang M, Stoner MW, Traba J, Corey C, et al. Loss of GCN5L1 in cardiac cells disrupts glucose metabolism and promotes cell death via reduced Akt/mTORC2 signaling. The Biochemical journal 2019;476(12):1713–24.
[14] Dong J, Xu X, Zhang Q, Yuan Z, Tan B. The PI3K/AKT pathway promotes fracture healing through its crosstalk with Wnt/β-catenin Experimental cell research 2020;394(1):112137.
[15] An Gj, Zhang Q. The research progress of traditional Chinese medicine in the treatment of osteoporosis guangming. J Chin Med 2023;38(18):3662–6 [In Chinese,English abstract].
[16] Hua-Wen L. Effects of Zhuangyao jianshen pills and liuwei dihuang pills in treatment of intractable strained low back pain. China Modern Medicine 2018;25(6):93–5 [In Chinese,English abstract].
[17] Zhao W. The impact of Zhuangyao jianshen pills on the healing of senile osteoporotic lumbar vertebral compression fractures. Lishizhen Medicine and Materia Medica 2011;22(11):2811–2 [In Chinese,English abstract].
[18] Huang D, Hou X, Zhang D, Zhang Q, Yan C. Two novel polysaccharides from rhizomes of Cibotium barometz promote bone formation via activating the BMP2/SMAD1 signaling pathway in MC3T3-E1 cells Carbohydrate polymers, vol. 231; 2020, 115732.
[19] Che CT, Wong MS. Ligustrum lucidum and its constituents: a mini-review on the anti-osteoporosis potential. Nat Prod Commun 2015;10(12):2189–94.
[20] Lai KD, Hu XX, Lu GS, Huang JY, Huang ZF, Yuan JT. Investigating the mechanism of total flavonoids from spatholobus suberectus Dunn in inhibiting osteoclast differentiation based on network pharmacology and experimental verification. Chinese Journal of Pharmacology and Clinical Chinese Medicine 2023;39(5):62–9 [In Chinese,English abstract].
[21] Liu Yl, Zhang YT, Gu Q, Teng XF, He L. Chemical constituents of the roots of Millettia speciosa champ and their inhibitory activity on osteoclast formation.

Natural Product Research and Development 2019;31(12):2046–2050+188 [In Chinese,English abstract].
[22] Shu-dong C, Fang-zheng L, Rui-min T, Si-ting Y. Lnvestigation on TCM pathogenesis,prevention and treatment of sarcopenia based on the theory of muscle soakage. In Chinese,English abstract 2023;35(9):71–5.
[23] Ma SY, Yang M, Wang JJ, Yang YJ. Research progress on bone metabolism and molecular mechanisms in accelerated aging SAMP6 mice Chinese Pharmacological Bulletin, vol. 1; 2024. p. 16–9 [In Chinese,English abstract].
[[24]] Deng WL. Principles for converting human doses to animal doses. Chinese Journal of Pharmacology and Clinical Chinese Medicine 2016;32(3):196–7 [In Chinese,English abstract].
[25] Rao VV, Mohanty A. Immunohistochemical identification of muscle fiber types in mice tibialis anterior sections. Bio-protocol 2019;9(20):e3400.
[26] Lee SJ. Quadrupling muscle mass in mice by targeting TGF-beta signaling pathways. PLoS One 2007;2(8):e789.
[27] Qaseem A, Hicks LA, Etxeandia-Ikobaltzeta I, Shamliyan T, Cooney TG, Cross Jr JT, et al. Pharmacologic treatment of primary osteoporosis or low bone mass to prevent fractures in adults: a living clinical guideline from the American college of physicians. Annals of internal medicine 2023;176(2):224–38.
[28] Zhao W. The impact of Zhuangyao jianshen pills on the healing of senile osteoporotic lumbar vertebral compression fractures lishizhen. Medicine and Materia Medica 2011;22(11):2811–2.
[29] Lung BE, Mowery ML, Komatsu DEE, Calcitriol [M]. StatPearls. Treasure Island (FL) ineligible companies. Disclosure: myles Mowery declares no relevant financial relationships with ineligible companies. In: Disclosure: david E Komatsu declares no relevant financial relationships with ineligible companies. StatPearls Publishing Copyright; 2024. StatPearls Publishing LLC. 2024.
[30] Ping JX, Liu GX, Zhu YY. The effect of calcitriol as an adjunct therapy on menopausal women with osteoporosis and its impact on bone metabolism markers. Maternal and Child Health Care of China 2024;3(8):29–32 [In Chinese,English abstract].
[31] Foretz M, Guigas B, Viollet B. Metformin: update on mechanisms of action and repurposing potential. Nat Rev Endocrinol 2023;19(8):460–76.
[32] Guarente L, Sinclair DA, Kroemer G. Human trials exploring anti-aging medicines Cell metabolism 2024;36(2):354–76.
[33] Sheng Z, Qian-yun F, Xue-li Z. Research progress and selection about animal models of primary osteoporosis and its related fracture Modern. Journal of Integrated Traditional Chinese and Western Medicine 2019;28(7):790–4 [In Chinese,English abstract].
[34] Kasai S, Shimizu M, Matsumura T, Okudaira S, Matsushita M, Tsuboyama T, et al. Consistency of low bone density across bone sites in SAMP6 laboratory mice. J Bone Miner Metabol 2004;22(3):207–14.
[35] Lane JM, Russell L, Khan SN. Osteoporosis Clinical orthopaedics and related research 2000;372:139–50.
[36] Farr JN, Khosla S. Cellular senescence in bone. Bone 2019;121:121–33.
[37] Zhong Y, Wang B, Chen W, Zhang H, Sun J, Dong J. Exploring the mechanisms of modified bu-shen-yi-qi decoction for COPD-related osteoporosis therapy via transcriptomics and network pharmacology approach. Drug Des Dev Ther 2023;17:2727–45.
[38] Zi-xuan Y, Yong-sheng Y. Research advancements in the role of mitochondria in osteoblast function. Central South Pharmacy 2023;21(12):3109–15.
[39] Moon DK, Kim BG, Lee AR, In Choe Y, Khan I, Moon KM, et al. Resveratrol can enhance osteogenic differentiation and mitochondrial biogenesis from human periosteum-derived mesenchymal. stem cells Journal of orthopaedic surgery and research 2020;15(1):203.
[40] Yan C, Shi Y, Yuan L, Lv D, Sun B, Wang J, et al. Mitochondrial quality control and its role in osteoporosis. Front Endocrinol 2023;14:1077058.
[41] Nakamura A, Kawakami K, Kametani F, Goto S. Dietary restriction increases protein acetylation in the livers of aged rats Gerontology 2013;59(6):542–8.
[42] Fukushima A, Alrob OA, Zhang L, Wagg CS, Altamimi T, Rawat S, et al. Acetylation and succinylation contribute to maturational alterations in energy metabolism in the newborn heart. Am J Physiol Heart Circ Physiol 2016;311(2):H347–63.
[43] Yun SH, Park JI. PGC-1α regulates cell proliferation and invasion via AKT/GSK-3β/β-catenin pathway in human colorectal cancer SW620 and SW480. Cells Anticancer research 2020;40(2):653–64.
[44] Delgado-Deida Y, Alula KM, Theiss AL. The influence of mitochondrial-directed regulation of Wnt signaling on tumorigenesis. Gastroenterology report 2020;8(3):215–23.
[45] Guo-ju L, Zhao-dong X, Yuan-fang L, Hui-can L. Gene expression microarray study on the antioxidative and anti-aging effects of Zhuangyao jianshen pills, vol. 4; 2006. p. 365–7.
[46] Sheng-ming S, Yong-bing Y, Xin-xin L, Hong-zhu L, Chang-ging C. Research progress on chemical constituents in Cibotium barometz and their pharmacological activities Drug Evaluation Research. In Chinese,English abstract 2016;39(3):489–92.
[47] Lulua G, Hongchena X, Lijina L, Mengmeng T, Yina H. Effect of Flemingia macrophylla mixed powder on improving bone function in rats. In Chinese,English abstract 2021;38:294–302.
[48] Ya-lan L, Yu-ting Z, Qiong G, Xi-feng T, Lin H. Chemical constituents of the roots of Millettia speciosa and their inhibitory effects on the formation of osteoclastic cell. Natural Product Research and Development 2019;12:2046–50 [In Chinese,English abstract].
[49] Kedao L, Xiaoxi H, Guoshou L, Jianyou H, Zhoufeng H, Jiantong Y. Mechanism of total flavonoids from SPATHOLOBI CAULIS in inhibiting osteoclast differentiation based on network pharmacology and experimental validation. Pharmacology and Clinics of Chinese Materia Medica 2023;39(5):62–9 [In Chinese,English abstract].
[50] Ying W, Jingru W, Wei Z, Wenjing Z. Research progress on pharmacological mechanisms of Cuscuta chinensis and lts extracts. Journal of Basic Chinese Medicine 2023;29(11):1961–4 [In Chinese,English abstract].
[51] Guihong W. Effects of HERBA TAXILLI on ovariectomized osteoporotic rats. Journal of Changzhi Medical College 2009;23(6):408–9.
[52] Yahui S, Jinin D, Chunya C, Jianxin L, An J, Weihua W. Screening and mechanism study of anti-inflammatory effective fraction of Kadsura coccinea. Tradit Chin Drug Res Clin Pharmacol 2022;33(12):1589–98.
[53] Zhang T, Sun W, Wang L, Zhang H, Wang Y, Pan B, et al. Rosa laevigata Michx. Polysaccharide ameliorates diabetic nephropathy in mice through inhibiting ferroptosis and PI3K/AKT pathway-mediated apoptosis and modulating tryptophan. Metabolism Journal of diabetes research 2023;2023:9164883.
[54] Grewal AK, Singh TG, Sharma D, Sharma V, Singh M, Rahman MH, et al. Mechanistic insights and perspectives involved in neuroprotective action of quercetin. Biomedicine & pharmacotherapy = Biomedecine & pharmacotherapie 2021;140:111729.
[55] Bian W, Xiao S, Yang L, Chen J, Deng S. Quercetin promotes bone marrow mesenchymal stem cell proliferation and osteogenic differentiation through the H19/miR-625-5p axis to activate the Wnt/β-catenin pathway. BMC complementary medicine and therapies 2021;21(1):243.
[56] Kedao L, Xiaoxi H, Guoshou L, Jianvou H, Zhoufeng H, Jiantono Y. Mechanism of total flavonoids from SPATHOLOBI CAULIS in lnhibiting osteoclast differentiation basedon network pharmacology and experimental validation. Pharmacology and Clinics of Chinese Materia Medica 2023;39(5):62–9 [In Chinese,English abstract].